06

Structure and mechanical properties of Cu-10Ag-37Zn soldering ribbons produced by rolling and melt quenching

© E.A. Sviridova,[1,2] S.V. Vasiliev,[1,2] A.N. Gangalo,[1,3] A.I. Yanchev,[1] Ya.S. Sokolovskii,[1] V.V. Burkhovetskii,[1] N.V. Chernyavskaya,[1] V.I. Tkatch[1]

Galkin Donetsk Institute for Physics and Engineering,
283048 Donetsk, Russia
[2]Donbass National Academy of Civil Engineering and Architecture,
286123 Makeyevka, Russia
[3]Institute for Physics of Mining Processes,
283048 Donetsk, Russia
e-mail: ksvir@list.ru

Received May 28, 2024
Revised September 27, 2024
Accepted October 8, 2024

Comparative analysis of the phase composition, structure and mechanical properties of ribbons of (wt.%) Cu-10Ag-37Zn soldering alloy (tradename PSr 10) with thicknesses of 110−130 μm produced by rolling and melt quenching methods with subsequent annealing were investigated by X-Ray diffraction, scanning electronic microscopy, microhardness measurements and three-point bending testing. The qualitative correlations between variations of the width of diffraction lines of FCC solid solutions based on Cu, Ag and BCC β-phase and changes of the plasticity and strength characteristics of the ribbons were established. The conditions for producing of the plastic ribbons which could withstand a full bend with a zero radius were determined, and it was established that the dominant factor determining plasticity was the level of microstrains which was proportional to the density of dislocations. The advantages of using of the melt quenching technique for plastic soldering ribbons producing were discussed.

Keywords: soldering alloy, ribbon, rolling, melt quenching, phase composition, microstrain, plasticity.

DOI: 10.61011/TP.2025.01.60511.193-24

Introduction

Solders based on Ag-Cu system, in particular ternary alloys Ag-Cu-Zn, are widely used in industry for soldering steel and bronze parts. In view of the high cost of silver, the important tasks are both the development of new compositions with a high copper content and the modification of the properties of standard materials, allowing expanding the range of their applications. Mechanical properties (strength and ductility) and temperature ranges of solidification are the most important characteristics of solder alloys. The level of mechanical properties is important not only for the strength of the joints of parts operated, for example, under stress or vibration conditions, but also for obtaining solder materials in various forms that are most convenient for practical applications, for example, in the form of thin rods, plates or tapes, necessary for many types of soldering and, in particular, for soldering in automatic modes. However, Ag-Cu-Ti-alloys with low silver content have high liquidus and solidus temperatures ($> 800^\circ$C) in the series of standard ternary solder alloys as stated in Ref. [1], and rolling of ribbons from such alloys requires several expensive process operations.

The quenching from the liquid state (solidification of the melt under cooling conditions at rates of $10^4 - 10^6$ K/s) is an alternative way to obtain solder alloys in low-dimensional forms with increased ductility. In particular, the use of the method of melt extraction with a rotating disk made it possible to obtain solders Cu-6P-4Sn and Cu-40Zn-5Sn (wt.%) in the form of wires with a diameter from 0.3 to 1.5 mm [2]. Ribbons of binary solder Cu-7.2P with a thickness of 0.2−0.35 mm were obtained using the method of lateral feeding of the melt onto a rotating crystallizer roll and these ribbons can be rolled into rings without fracture [3]. Solder alloys Ag-Cu-Ti [1] and the eutectic alloy $Al_{77}Ge_{23}$ [4] were obtained using a more efficient quenching spinning method — solidification of a thin layer of melt on the outer surface of a rotating quenching roll in a ribbon shape (with thickness from 20 to 100 μm). Experiments have shown that rapidly cooled Ag-Cu-Ti ribbons containing 20% Ag can be used as a replacement for solder containing 60% Ag [1], and Al-Ge alloy ribbons can replace expensive solders of Au-Si system for connecting silicon chips to a metallic substrate [4]. In addition to the rapidly cooled ribbons of brazing alloys with a crystalline structure, ribbons of alloys with an amorphous structure are also used for soldering [5]. A common characteristic of rapidly cooled wires and ribbons is a significantly increased plasticity compared to the raw materials, which is caused by not only the shape factor, but also, mainly, with structural changes. An additional advantage of melt quenching methods is the single-stage nature of the technological process for obtaining the final product.

Taking into account the results of the cited above studies, it seems interesting to apply the method of quenching from a liquid state to obtain solder ribbons of the ternary system Cu-Ag-Zn and to compare their structure and mechanical properties with the characteristics of the ribbon samples obtained by rolling using conventional technology. The alloy PSr 10 (Cu-10Ag-37Zn (wt.%)) was chosen for study in this paper which contains a minimum amount of silver and melts in the range of 822−850°C within a series of standard solders of the ternary system Cu-Ag-Zn, and the most common melt spinning technique used in Refs. [1,4] was chosen as a quenching method.

1. Materials and methods of the experiment

The ribbon-shaped samples of Cu-10Ag-37Zn solder were obtained by cold rolling and melt quenching. A ribbon obtained by extrusion of an alloy heated to a temperature of 750−780°C through a flat matrix with a cross section of 2×20 mm was used as a rolling billet. The billet was rolled to a thickness of $120 \pm 8\,\mu$m in several passes with two intermediate annealings at a temperature of 450°C for 30 minutes. The melt spinning method was used to obtain the ribbons quenched from a liquid state. An ingot consisting of solder alloy pieces with a total weight of about 15 g was melted by induction heating in a quartz tube with a diameter of 18 mm with a slit hole with dimensions 5×1 mm in the bottom part. The melt was heated to a temperature of 900°C (about 50 degrees above the liquidus temperature) and ejected by Ar gas at a pressure of 20 kPa onto the outer surface of a rotating copper roller, the linear velocity of which was approximately 7.5 m/s. The ribbon obtained using these casting conditions had a width of 5 mm and a thickness of $115 \pm 5\,\mu$m. The estimation of its cooling rate (q) by thickness h using the empirical equation $\log_{10}(q) = 10.8 - 3.1 \cdot \log_{10}(h)$ [6] gives the value of $2.6 \cdot 10^4$ K/s. The heat treatment of the rolled and quick-cooled ribbons was carried out in vacuum by holding for half an hour at a temperature of 500 ± 5 °C.

The structure of the ribbons was studied by X-ray and scanning electron microscopy. X-ray examinations were performed on an automated diffractometer DRON-3M in cobalt radiation using a Fe filter. The angular positions of the reflexes, their integral intensity, and half-width B were determined from diffraction patterns. The ratio of the reflection intensities of (111) FCC of solid solutions based on Cu (α), Ag (α') and (110) BCC of βphases located in a narrow range of diffraction angles was used to estimate the relative amount of phases. The values of the fine structure parameters (sizes of coherently scattering domains (CSD) $L = \frac{\lambda}{\beta_L \cos\theta}$ and microstresses $\langle\varepsilon^2\rangle^{1/2} = \frac{\beta_S}{2\sqrt{2}\pi \operatorname{tg}\theta}$, the values of which are proportional to the dislocation density [7]) were estimated by the half-widths of the corresponding lines, determined taking into account the instrumental broadening [8]. Here θ is the angular position of reflexes, β_L and β_S are contributions to broadening due to the size of CSD and microstresses, respectively. The values of β_L and β_S were estimated by using the results of a full-profile analysis of the lines of the Al standard recorded under identical recording conditions, approximated by Gaussian functions and adjusted for the magnitude of the angular multiplier and the deviation of the sample plane from the axis of the goniometer [9,10]. The angular dependence of the line width of the standard b obtained as part of this analysis was approximated by the Caglioti equation [11], which has the form $b = 0.1675 + 0.2031\tan(\theta) + 0.0312\tan^2(\theta)$ for the shooting conditions used in the work. The physical broadenings were calculated, respectively β_L and β_S as $(B^2 - b^2)^{1/2}$ based on the measured values of the half-widths of the lines (111) and (220) of solid solutions and lines (110) and (220) of β-phase, the profiles of which were satisfactorily approximated by Gaussian functions.

Pieces of the ribbons were placed in a cage and filled with epoxy resin, after polymerization of which the surface of the samples was subjected to mechanical grinding and polishing for conducting structural studies and measuring microhardness. A conductive carbon layer was deposited on the surface of the polished section by sputtering in the VUP-5A installation before examining the microstructure and determining the elemental composition of the structural components.

The microstructure on the polished surface of the samples was studied using JSM6490LV scanning electron microscope (SEM) equipped with INCA Wave FETx3 energy-dispersive X-ray spectrometer. The differences in the structural components were revealed by the contrast of the images (by atomic number) using a backscattered electron detector. The quantitative analysis of the element composition in the detected phases was carried out by the electron probe microanalysis using a wave dispersion detector.

The strength characteristics of the ribbon samples were evaluated based on the microhardness values, and the plasticity was evaluated using the results of three-point bending tests. Microhardness was measured using a standard microhardness tester PMT-3 with 136° diamond pyramid indenter with a load of 0.49 N (holding time of 10 s) and was determined as the average value of ten measurements. The ribbons were tested according to the three-point bending scheme using a laboratory setup for measuring small samples, described in Ref. [12], with a distance between the supports 2.015 ± 0.005 mm, mounted on a plate of measuring microscope MMI-2. The measurements were carried out in accordance with the requirements of GOST R 56810-2015 and the following properties were determined using the obtained „stress-strain“ diagrams:

— modulus of elasticity at transverse bending, $E_b = mL^3/(4bh^3)$,

— deformation on the outer surface of the sample ($\varepsilon = 6\delta h/L^2$),

— fracture stress of the sample, $\sigma = \frac{3FL}{2bh^2}\left[1 + 6\left(\frac{\delta}{L}\right)^2 - -4\left(\frac{\delta d}{L^2}\right)\right]$, where m is the slope of the initial linear part of

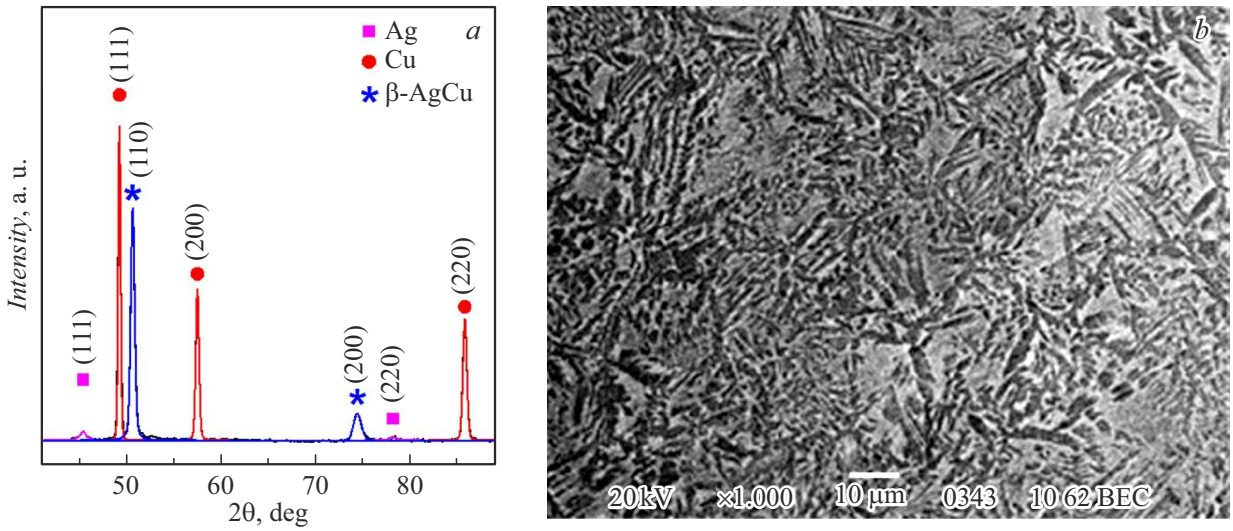

Figure 1. Diffraction pattern (a) and microstructure (b) of a rapidly cooled ribbon of Cu-10Ag-37Zn alloy.

the load-deviation curve, F is the load, L is the distance between the supports, b and h is the width and thickness of the sample, respectively, and δ is the deflection of the central part of the sample.

The method of deformation of a U-shaped sample between two plates of a micrometer was used for an additional evaluation of the plasticity of the ribbon samples [13]. The relative deformation ε_f at which the samples were fractured was defined in this method as $\varepsilon_f = t/(d-t)$, where t was the thickness of the ribbon, d was the distance between the plates at the moment destruction.

2. Results and discussion

X-ray studies of the structure of Cu-10Ag-37Zn rapidly cooled ribbon (Fig. 1, a) have shown that it consists of three phases — two solid solutions based on copper (α) and silver (α'), as well as β-phase (Hume-Rothery phase with a BCC lattice). Approximate quantitative analysis of the diffraction pattern in Fig. 1, a (without taking into account differences in atomic factors) showed that the β-phase (54%) is the dominant phase, and the relative fractions of solid solutions based on Cu (α) and based on Ag (α') were 42 and 4%, respectively.

Electron microscopic studies reveal two structural constituents (Fig. 1, b). The electron probe microanalysis found that the dark structural component had a composition of ($\pm$1%) 59Cu-34Zn-7Ag, and the light structural component has a composition of 52Cu-39Zn-9Ag, while the average alloy composition corresponded to the nominal composition. The microstructure shown in Fig. 1, b similar in appearance to the microstructure of solder Cu-20Zn-43Ag [14] and, most likely, was formed by nucleation and growth of primary dendrites of α-solid solution during quick cooling of the melt followed by solidification of the ternary eutectic present in the experimental and calculated ternary melting diagrams [15,16]. The structure obtained by quenching from liquid state is thermodynamically nonequilibrium, since the composition of the alloy studied in this paper in the temperature range of $350-670^\circ$C is in the two-phase region $\alpha+\beta$ closer to the boundary of region of α-solid solution according to the experimental and calculated isothermal sections of the ternary diagram Cu-Ag-Zn [14,16,17].

The ribbon obtained by rolling also has a three-phase structure (Fig. 2, a) with a slightly different phase ratio: 67 and 7% of α- and α'-solid solutions based on Cu and Ag, respectively, and 26% of β-phases, however with significantly different morphology of the structure (Fig. 2, b). As in the rapidly cooled ribbon, the dark structural component is enriched by copper (58Cu-34Zn-7Ag), and the light structural component is enriched by zinc and silver (50Cu-39Zn-11Ag). In view of the complex thermal history of the rolled ribbon, it seems incorrect to judge about the mechanism of crystallization, however, the similarity (within the microanalysis error limits) of the chemical compositions of the dark and light components in the ribbons obtained by rolling and casting suggests their common nature. It can be concluded based on this assumption that the relative fraction and grain sizes of α-solid solution in the rolled ribbon are significantly higher than in the rapidly cooled one, and the fraction of β-phase in the eutectic is lower. It should also be noted that the intensity of FCC lines (220) of α- and α'-solid solutions is higher than the intensity of lines (111), and the line (200) of β-phase is more intensive than the line (110) (Fig. 2, a), which is a consequence of the texture formed during the rolling process.

Samples of rolled and rapidly cooled ribbons were subjected to three-point bending tests for evaluation of the mechanical characteristics. The tests showed that the deformation diagram of the rolled ribbon (Fig. 3) had a classical shape — the initial linear part of the elastic deformation was followed by the plastic deformation of the sample and failure after reaching a certain maximum value. The

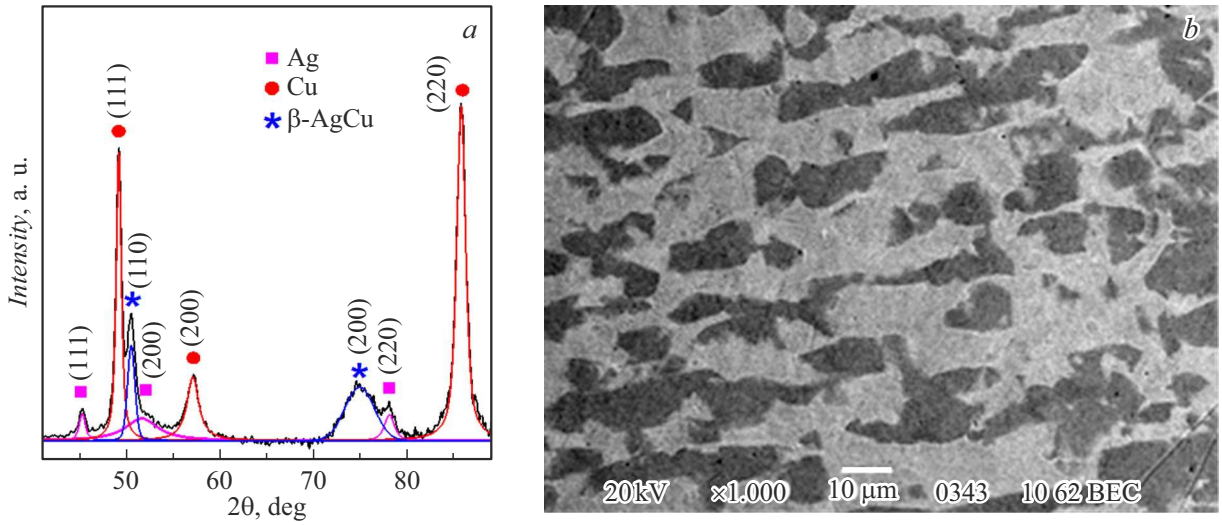

Figure 2. Diffraction pattern (a) and microstructure (b) of the rolled ribbon of Cu-10Ag-37Zn alloy.

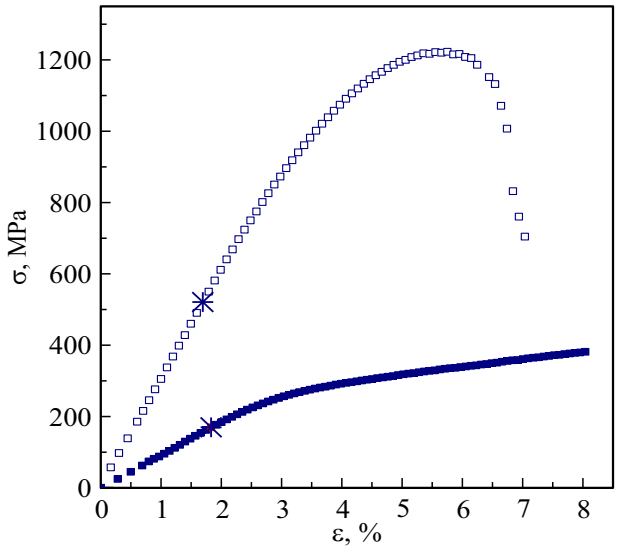

Figure 3. Diagrams of three-point bending tests of Cu-10Ag-37Zn alloy ribbons obtained by rolling (light symbols) and quenching from a melt (solid symbols). The proportionality limits are marked with asterisks.

mechanical characteristics of the ribbon sample obtained by rolling: modulus of elasticity $E_b = 31$ GPa, limit of proportionality $\sigma_{el} = 520$ MPa, fracture stress $\sigma_m = 1222$ MPa, plastic deformation ε_{pl}, equal to the difference between the total deformation ε_f and the elastic deformation ε_{el} was approximately 4.5%. Such a low level of plasticity limits the possibilities of shaping the rolled ribbon, in particular, folding it into rings with a diameter of less than 20 mm.

The three-point bending diagram of a rapidly cooled ribbon has a fundamentally different shape and consists of two almost linear parts (Fig. 3). The initial part of a rolled ribbon corresponds to elastic deformation, and the ribbon continues to deform after exceeding the proportionality limit until it reaches a stop without breaking, which indicates a relatively high plasticity. This is confirmed by the results of bending tests of the rapidly cooled ribbon between micrometer plates [13], which showed that it can withstand a full 180 bend° with a zero radius without signs of fracture. As follows from the diagram, the values of the bending modulus (9 GPa) and the limit of proportionality (170 MPa) of the rapidly cooled ribbon are significantly lower than the bending modulus and limit of proportionality of the rolled ribbon. The rapidly cooled ribbon of Cu-10Ag-37Zn alloy also has a lower microhardness (1.81 ± 0.05 GPa) compared to the rolled ribbon (2.5 ± 0.1 GPa). Nevertheless, this value is noticeably higher than the hardness of 50Cu-25Ag-25Zn solder (1.06 GPa) [18] and hardness of the majority of four-part alloys 25Ag-(39–46)Cu-25Zn-(3–10)Sn, the hardness of which is in the range of 1.1–2.9 GPa [19].

It was of interest to study the effect of annealing on the structure and mechanical properties because both rolled and rapidly cooled ribbons are in thermodynamically nonequilibrium states. 30 min regime was chosen at 500°C ($\approx 0.7T_{liq}$) at this stage of the study, close to that used to remove the work-hardening in rolled of Cu-10Ag-37Zn solder. X-ray studies, the results of which are shown in Fig. 4, showed that the relative amount of α-solid solution in both annealed ribbons significantly increases (up to 82 and 84% in rapidly cooled and rolled ribbons, respectively) at the expense of the decrease of the fraction of β-phase in these ribbons down to 5.1 and 9.8%, besides this the width of reflexes located at angles 2θ higher than 70° is reduced.

Electron microscopic studies of the microstructure of heat-treated ribbons have shown (Fig. 5) that annealing leads to an alignment of the grain sizes of the dark phase enriched by copper in rolled and rapidly cooled samples, however, the morphology of the light phase enriched by silver and zinc significantly differs. In fact, crystals of the light phase (ternary eutectic) with clearly defined

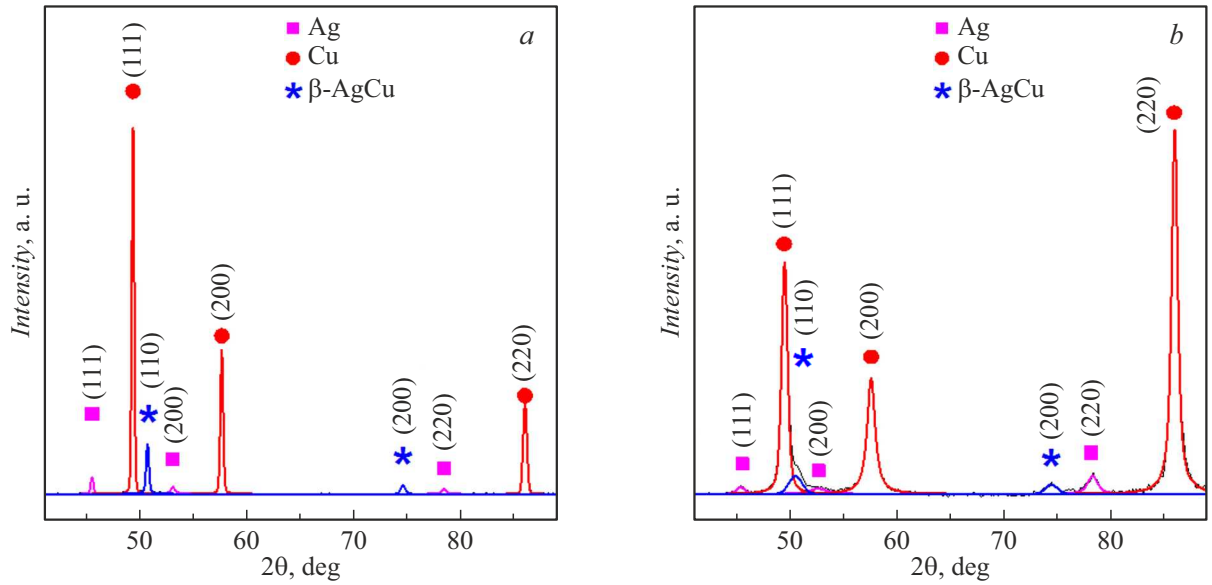

Figure 4. Diffraction patterns of rapidly cooled (a) and rolled (b) ribbons of Cu-10Ag-37Zn alloy after isothermal annealing for 30 min at 500°C.

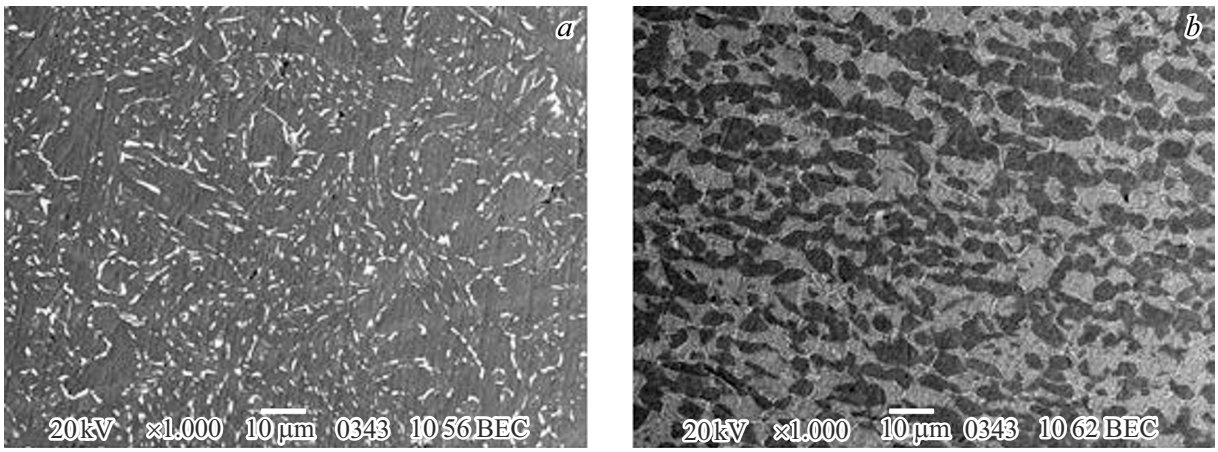

Figure 5. Microstructure of rapidly cooled (a) and rolled (b) ribbons of Cu-10Ag-37Zn alloy after isothermal annealing for 30 min at 500°C.

boundaries are distributed over the volume in the rolled sample (the grain size is significantly reduced) (Fig. 5, b). The light phase is located along the grain boundaries of the dark phase in the sample of the ribbon obtained by rapid solidification (Fig. 5, a).

As expected, the structural changes led to a change of the mechanical properties, especially in the rolled ribbon (Fig. 6). The proportionality limit significantly decreased (from 520 to 379 MPa) despite the fact that the elastic modulus of the rolled ribbon after annealing became slightly higher (32 GPa). In addition, the stress-strain diagram has lost the maximum due to the failure of the sample, which indicates an increase of the level of plasticity. At the same time, the annealing of the rapidly cooled ribbon did not affect the nature of the bending diagram, but only led to a slight decrease of the elastic modulus (from 9 to 6.5 GPa) and the proportionality limit (from 170 to 101 MPa). Additional assessments of plasticity showed that the annealed samples of rolled and rapidly cooled ribbons withstood a complete bend between the micrometer plates without any signs of fracture. As expected, annealing led to a decrease of the microhardness of the rapidly cooled and rolled ribbons to 1.58 ± 0.05 and 1.7 ± 0.1 GPa, respectively.

It follows from the above experimental results that plastic (withstanding a full bend with a zero radius) ribbons with a thickness of $110 - 130\,\mu$m of Cu-10Ag-37Zn solder alloy can be obtained either by annealing the rolled ribbon or directly from the melt by cooling a thin layer on the outer surface of a rotating quenching roll. In view of the practical importance of the problem of obtaining plastic ribbons of solder alloys, it seemed interesting to establish the structural parameters of the studied alloy, which determine plasticity.

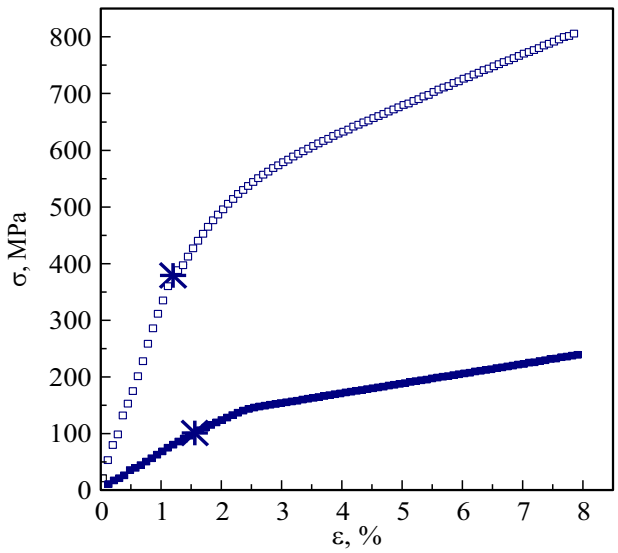

Figure 6. Diagrams of three-point bending tests of annealed samples of rolled (light symbols) and rapidly cooled (solid symbols) ribbons of Cu-10Ag-37Zn alloy. The proportionality limits are marked with asterisks.

The X-ray data demonstrate that annealing of the rolled ribbon leads to a change of the quantitative phase ratio (an increase of the fraction of α-solid solution based on copper and a decrease of the relative amount of β-phase) and a change of the angular positions and width of the diffraction lines. Experimentally measured angular displacements of the lines, indicating changes in the composition of the phases, did not exceed the accuracy limits of the diffraction patterns shown in Figs. 1, 2 and 4, and for this reason they were not taken into account in the subsequent analysis. The contribution of changes of the fraction of α'-solid solution based on Ag was also not taken into account since its the value was less than 10%, and its changes did not exceed 4%.

Analysis of the diffraction patterns showed that both the sizes of the CSD of crystals of α-solid solution and β-phase (79 and 29 nm) and the level of microstresses ($4.1 \cdot 10^{-3}$ and $1.7 \cdot 10^{-2}$) is significantly higher in the rolled sample than in the rapidly cooled ribbon (19.4 and 13 nm and $1.2 \cdot 10^{-3}$ and $4.2 \cdot 10^{-3}$, respectively). Taking into account that the grinding of both the grain and subgrain structures contributes to the hardening [20] and, consequently, to a decrease of ductility, the data obtained suggest that the low ductility of the rolled ribbon of Cu-10Ag-37Zn alloy is caused by the high level of microstresses of the lattices of α- and β-phases. Annealing of the rolled ribbon leads to an increase of the CSD of crystals of α-solid solution and β-phase (up to ≥ 200 and 80 nm, respectively), and to a decrease of the level of microstresses in these phases (up to $2.1 \cdot 10^{-3}$ and $5.8 \cdot 10^{-3}$), which, as shown above, is accompanied by a significant increase of plasticity. The level of microstresses is also reduced in the annealed, rapidly cooled ribbon (to $6.5 \cdot 10^{-4}$ in the α-solid solution and to $1.8 \cdot 10^{-3}$ in the β-phase), but the size of the CSD of crystals of these phases remains small (18.5 and 8.0 nm, respectively). It should be noted that the higher level of microstresses in crystals of the β-phase compared to crystals of a solid solution based on copper is most likely due to the fact that the β-phase is an integral part of eutectic colonies. The levels of microstresses of α-solid solution in the ribbons of Cu-10Ag-37Zn alloy found in the paper are slightly higher than in crystals of the solid solution based on Al in deformed samples of Al-1.47Cu-0.34Zr alloy ($(4.4 - 6.8) \cdot 10^{-4}$) [21], because, α-solid solution contains up to 10% of alloying elements according to the phase diagram of Ag-Cu-Zn system [14].

It follows from the results of the comparative analysis of the structure of the ribbons of Cu-10Ag-37Zn solder alloy obtained by rolling and quenching from the liquid state, that the processes of treatment of the studied ribbons can be arranged in the following sequence according to their degree of structural nonequilibrium: rolling, rolling+annealing, quenching from melt and quenching from melt+annealing. It is noteworthy that the values of the proportionality limit of the ribbons measured by three-point bending tests decrease in the same sequence: 520, 379, 170 and 101 MPa and microhardness values change almost similarly: 2.5 ± 0.3, 1.7 ± 0.1, 1.81 ± 0.05, 1.58 ± 0.05 GPa.

Despite the fact that the methods used in this study did not allow a quantitative comparison of the levels of plasticity of the ribbons, the analysis of the above results allows making the following considerations about the reasons of variations in the plasticity of the three-phase structure of Cu-10Ag-37Zn solder alloy. Since the structural changes of the rolled ribbon during annealing, leading to an increase of plasticity, include a decrease of the size of the CSD, the level of microstresses and the concentration of β-phase, and the ribbon obtained by quenching from the melt, with larger CSD and with a high content of β-phase, has high plasticity, it follows from the comparison of these facts that the level of microstresses or the dislocation concentration is the dominant factor determining the plasticity of ribbons.

It also follows from the results of the studies that the plastic ribbons of Cu-10Ag-37Zn solder alloy with a thickness of $110-130\,\mu$m can be obtained both by the traditional rolling method followed by annealing, and directly by rapid cooling of the melt. However, accounting the single-stage nature of the production of a rapidly cooled ribbon, the high productivity of the melt spinning method and its environmental safety, as well as the dispersed nature of the cast microstructure, which facilitates melting and increases the uniformity of the joint structure, the process of producing of ribbons directly from the melt seems preferable. It should be noted that one of the advantages of the spinning method used on an industrial scale is also the possibility of changing the geometric parameters of the ribbons in a fairly wide range by adjusting the parameters of the casting process.

Conclusion

The following conclusions can be made based on the results of studies of the structure and measurements of the

mechanical characteristics of Cu-10Ag-37Zn solder ribbons with a thickness of $110-130\,\mu$m obtained by metal forming (hot pressing and rolling with intermediate annealing) and directly by the melt by spinning:

1. It was found that Cu-10Ag-37Zn solder ribbon, obtained for the first time by rapid cooling of the melt at a rate of $2.4 \cdot 10^4$ K/s, has the same phase composition (FCC solid solutions based on Cu (α) and Ag (α') and that based on BCC of Hume-Rothery β-phase), as well as the ribbon obtained by rolling, but with a lower content of α-solid solution, increased content of β-phase and a more finely dispersed structure.

2. Three-point bending tests have shown that the rolled ribbon fails after 4.6% deformation, while the ribbon obtained by quenching from the melt not only deforms without fracture, but also withstands a full 180° bending with a zero radius. The rolled ribbon acquires similar signs of plasticity after half an hour of annealing at 500°C.

3. From a comparison of the values of fine structure parameters (CSD sizes and microstresses) with the results of plasticity measurements, it follows that the increase of plasticity of ribbon samples is due to a decrease of the magnitude of microstresses in α-solid solution and β-phase (from $4.1 \cdot 10^{-3}$ and $1.7 \cdot 10^{-2}$ to $2.1 \cdot 10^{-3}$ and $5.8 \cdot 10^{-3}$, respectively) to a level comparable to the microstresses in α and β-phases of the rapidly cooled ribbon ($1.2 \cdot 10^{-3}$ and $4.2 \cdot 10^{-3}$).

4. The use of the microstress level as an indicator of the degree of nonequilibrium suggests that the structure of a relatively brittle rolled ribbon with the highest values of microhardness and the limit of proportionality (2.5 ± 0.3 GPa and 520 MPa, respectively) is characterized by the greatest deviation from equilibrium, and the structure of a plastic annealed rapidly cooled ribbon is the closest to equilibrium having minimum levels of microhardness and limit of proportionality (1.58 ± 0.05 GPa and 101 MPa, respectively).

5. The single-stage nature of the process, the high productivity of the melt spinning method and the acceptable level of mechanical characteristics (microhardness of 1.81 GPa combined with high ductility) of the rapidly cooled ribbon of commercial Cu-10Ag-37Zn solder alloy indicate the prospects of using this method to produce plastic solder alloy ribbons.

Conflict of interest

The authors declare that they have no conflict of interest.

References

[1] P. Duhaj, P. Sebo, P. Svec, D. Janičkovič. Mater. Sci. Eng. A, **271**, 181 (1999). DOI: 10.1016/S0921-5093(99)00275-0

[2] V.A. Vasiliev, B.S. Mitin, I.N. Pashkov, I.V. Rodin. Mater. Sci. Eng. A, **133**, 742 (1991). DOI: 10.1016/0921-5093(91)90176-N

[3] S.A. Tavolzhanskii, I.N. Pashkov, G.A. Metallurgist, **59**, 843, (2016). DOI: 10.1007/s11015-016-0182-1

[4] L. Illgen, H. Muhlbach, W. Loser, H.-G. Lindenkreuz, E. Alius, D. Ruhlicke, M. Muller. Mater. Sci. Eng. A, **133**, 738 (1991). DOI: 10.1016/0921-5093(91)90175-m

[5] K.B. Kim, J.G. Lee, J.K. Lee, S.W. Son, M.K. Lee, S.J. Kim, C.K. Rhee. Mater. Lett., **62** (30), 4483 (2008). DOI: 10.1016/j.matlet.2008.08.019

[6] V.I. Tkatch, A.L. Limanovskii, S.N. Denisenko, S.G. Rassolov. Mater. Sci. Eng. A, **323**, 91 (2002). DOI: 10.1016/S0921-5093(01)01346-6

[7] G.K. Williamson, R.E. Smallman. Philos. Mag., **1** (1), 34 (1956). DOI: 10.1080/14786435608238074

[8] S.S. Gorelik, Yu.A. Skakov, L.N. Rastorguev. *Rentgenograficheskiy i elektronno-opticheskiy analiz* (M., MISIS, 2002) (in Russian).

[9] E.A. Sviridova, T.V. Tsvetkov, V.M. Tkachenko, A.I. Limanovsky, V.N. Sayapin, S.V. Vasiliev, V.I. Tkatch. Tr. Kol'skogo NC RAN. Seriya: Tekhnicheskie nauki, **13** (1), 223 (2022) (in Russian). DOI: 10.37614/2307-5252.2021.2.5.045

[10] S.V. Vasiliev, T.V. Tsvetkov, E.A. Sviridova, V.M. Tkachenko, A.I. Limanovsky, V.N. Sayapin, V.I. Tkatch. Fiz. tekhn. vys. davl., **32** (1), 8 (in Russian). (2022). http://www.donfti.ru/main/wp-content/uploads/2022/03/1-Vasilev.pdf

[11] G. Caglioti, A. Paoletti, F.P. Ricci. Nuclear Instrum., **3**, 223 (1958). DOI: 10.1016/0369-643X(58)90029-X

[12] S.V. Vasiliev, E.A. Sviridova, A.I. Limanovsky, V.M. Tkachenko, T.V. Tsvetkov, V.V. Burkhovetsky, V.N. Varyukhin, V.I. Tkatch. Physics of the Solid State, **65** (12), 2131 (2023).

[13] F.E. Luborsky, J.L. Walter. J. Appl. Phys., **47** (8), 3648 (1976). DOI: 10.1063/1.323173

[14] S.P. Dimitrijević, D. Manasijević, Z. Kamberović, S.B. Dimitrijević, M. Mitrić, M. Gorgievski, S. Mladenovic. J. Mater. Eng. Perform., **27**, 1570 (2018). DOI: 10.1007/s11665-018-3258-1

[15] M.E. Drits, N.R. Bochvar, L.S. Guzey, E.V. Lysova, E.M. Padezhnova, L.L. Rokhlin, N.I. Turkina. *Dvojnye i mnogokomponentnye sistemy na osnove medi*: spravochnik (Nauka, M., 1979) (in Russian)

[16] V.T. Witusiewicz, S.G. Fries, U. Hecht, A. Drevermann, S. Rex. Int. J. Mat. Res., **97**, 556 (2006). DOI: 10.3139/146.101272

[17] Y.A. Chang, D. Goldberg, J.P. Neumann. Phys. Chem. Ref. Data, **6**, 621 (1977). DOI: 10.1063/1.555555

[18] Y. Xiao, L.-H. Lang, W.-C. Xu. Trans. Nonferrous Met. Soc. China, **31**, 475 (2021). DOI: 10.1016/S1003-6326(21)65510-3

[19] Ł.J. Wierzbicki, W. Malec, J. Stobrawa, B. Cwolek, B. Juszczyk. Archiv. Metall. Mater., **56**, 147 (2011). DOI: 10.2478/v10172-011-0017-9

[20] V.A. Mikheev, L.V. Zhuravel. Izv. vuzov. Tsvetnaya metallurgiya, **3**, 56 (2016). DOI: 10.17073/0021-3438-2016-3-56-64

[21] T.S. Orlova, D.I. Sadykov, M.Yu. Murashkin, V.U. Kazykhanov, N.A. Enikeev. Phys. Solid State, **63** (10), 1572 (2021) (in Russian). DOI: 10.21883/FTT.2021.10.51408.104

Translated by A.Akhtayamov